Leis, J., & Jentoft, J. (1983) *J. Virol. 48*, 361-369.
Lohman, T. M., deHaseth, P. L., & Record, M. T., Jr. (1980) *Biochemistry 19*, 3522-3530.
Meric, C., & Spahr, P.-F. (1986) *J. Virol. 60*, 450-459.
Prats, A. C., Sarih, L., Gabus, C., Litvak, S., Keith, G., & Darlix, J. L. (1988) *EMBO J. 7*, 1777-1783.
Roberts, W. J., Elliott, J. E., McMurray, W. J., & Williams, K. R. (1988) *Peptide Res. 1*, 74-80.
Secnik, J., Wang, Q., Chang, C.-M., & Jentoft, J. E. (1990) *Biochemistry 29*, 7991-7997.
Smith, B. J., & Bailey, J. M. (1979) *Nucleic Acids Res. 7*, 2055-2072.
Wang, J. L., & Edelman, G. M. (1971) *J. Biol. Chem. 246*, 1185-1191.

Role of Magnesium Ion in the Interaction between Chromomycin A_3 and DNA: Binding of Chromomycin A_3–Mg^{2+} Complexes with DNA

Palok Aich,[‡] Ranjan Sen,[‡] and Dipak Dasgupta*[,‡]

Crystallography and Molecular Biology Division, Saha Institute of Nuclear Physics, I/AF, Bidhan Nagar, Calcutta 700 064, India

Received July 16, 1991; Revised Manuscript Received December 10, 1991

ABSTRACT: Chromomycin A_3 is an antitumor antibiotic which blocks macromolecular synthesis via reversible interaction with DNA template only in the presence of divalent metal ions such as Mg^{2+}. The role of Mg^{2+} in this antibiotic–DNA interaction is not well understood. We approached the problem in two steps via studies on the interaction of (i) chromomycin A_3 and Mg^{2+} and (ii) chromomycin A_3–Mg^{2+} complex(es) and DNA. Spectroscopic techniques such as absorption, fluorescence, and CD were employed for this purpose. The results could be summed up in two parts. Absorption, fluorescence, and CD spectra of the antibiotic change upon addition of Mg^{2+} due to complex formation between them. Analysis of the quantitative dependence of change in absorbance of chromomycin A_3 (at 440 nm) upon input concentration of Mg^{2+} indicates formation of two types of complexes with different stoichiometries and formation constants. Trends in change of fluorescence and CD spectroscopic features of the antibiotic in the presence of Mg^{2+} at different concentrations further corroborate this result. The two complexes are referred to as complex I (with 1:1 stoichiometry in terms of chromomycin A_3:Mg^{2+}) and complex II (with 2:1 stoichiometry in terms of chromomycin A_3:Mg^{2+}), respectively, in future discussions. The interactions of these complexes with calf thymus DNA were examined to check whether they bind differently to the same DNA. Evaluation of binding parameters, intrinsic binding constants, and binding stoichiometry, by means of spectrophotometric and fluorescence titrations, shows that they are different. Distinctive spectroscopic features of complexes I and II, when they are bound to DNA, also support that they bind differently to the above DNA. Measurement of thermodynamic parameters characterizing their interactions with calf thymus DNA shows that complex I–DNA interaction is exothermic, in contrast to complex II–DNA interaction, which is endothermic. This feature implies a difference in the molecular nature of the interactions between the complexes and calf thymus DNA. These observations are novel and significant to understand the antitumor property of the antibiotic. They are also discussed to provide explanations for the earlier reports that in some cases appeared to be contradictory.

Chromomycin A_3 ($CHRA_3$,[1] structure shown in Figure 1; Thiem & Meyer, 1979; Van Dyke & Dervan, 1983) is an antitumor antibiotic produced from *Streptomyces griseus* (Gause, 1975). This antibiotic, along with structurally related antibiotics like mithramycin and olivomycin, belongs to the aureolic acid group (Bakhara et al., 1968; Thiem & Meyer, 1979; Calabresi & Parks, 1985). They bind to double-stranded DNA, thereby blocking its function as a template for DNA and RNA polymerases (Wakisaka et al., 1963; Ward et al., 1965; Calabresi & Parks, 1985). The reversible interaction with DNA leading to the inhibitory effects on macromolecular synthesis requires the presence of a divalent metal ion, Mg^{2+} (Kersten et al., 1966; Goldberg & Friedmann, 1971). Optical and NMR spectroscopy (Ward et al., 1965; Behr et al., 1969; Hayasaka & Inoue, 1969; Nayak et al., 1973, 1975; Shashiprabha, 1979; Berman et al., 1985; Keniry et al., 1987; Kam et al., 1988; Gao & Patel, 1989, 1990; Banville et al., 1990a,b), enzymatic and chemical footprinting (Van Dyke & Dervan, 1983; Fox & Howarth, 1985; Fox & Waring, 1986; Cons & Fox, 1989), and hydrodynamic studies (Behr & Hartmann, 1965; Kersten et al., 1966; Waring, 1970; Cobreros et al., 1982) were carried out to understand the molecular basis of $CHRA_3$–DNA interaction in the presence of Mg^{2+}. Spectrophotometric methods indicated a GC base specificity of the antibiotic; the origin of the base specificity was ascribed to hydrogen bonding between a potential site in the antibiotic and an amino group of the guanine base in GC residues (Goldberg & Friedmann, 1971). Footprinting studies using

* To whom correspondence should be addressed.
‡ Present address: Biophysics Division, Saha Institute of Nuclear Physics, 37 Belgachia Road, Calcutta 700 037, India.

[1] Abbreviations: CD, circular dichroism; $CHRA_3$, chromomycin A_3; FPA, fluorescence polarization anisotropy; MTR, mithramycin; poly(dG-dC), double-stranded alternating copolymer, poly(dG-dC)·poly(dG-dC); poly(dG-me^{5}dC), double-stranded alternating copolymer, poly(dG-me^{5}dC)·poly(dG-me^{5}dC).

0006-2960/92/0431-2988$03.00/0

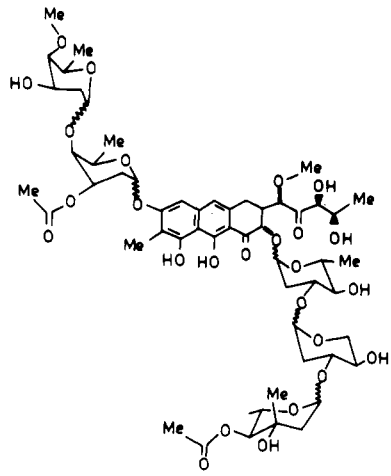

FIGURE 1: Structure of chromomycin A_3 (van Dyke & Dervan, 1983). The central aglycon ring is referred to as chromomycinone.

methidiumpropyl-EDTA (MPE), DNase I, and hydroxyl radical confirmed this broad base selectivity and further suggested that the antibiotic preferentially recognises a specific dinucleotide step (Van Dyke & Dervan, 1983; Fox & Howarth, 1985; Fox & Waring, 1986; Cons & Fox, 1989). NMR studies on the interaction of the antibiotic with poly(dG-dC), fragments of calf thymus DNA, and several oligonucleotides led to contradictory conclusions regarding the nature of binding. One of them favored an intercalative mode of binding of the antibiotic (Berman et al., 1985). The rest of the reports emphasized an external binding mode. However, they differed on the nature of the groove via which it binds to DNA, major or minor (Berman et al., 1985; Keniry et al., 1987; Kam et al., 1988; Gao & Patel, 1989, 1990; Banville et al., 1990a). A couple of these studies proposed a geometry of the antibiotic–oligonucleotide complex (Gao & Patel, 1990; Banville et al., 1990b). The results from these studies suggested that binding of $CHRA_3$ leads to perturbation of B-DNA structure of the oligomer at the binding site. Hydrodynamic studies such as sedimentation profiles of circular DNA in the presence of increasing concentrations of the antibiotic indicated an external mode of binding of the antibiotic (Waring, 1970). On the other hand, kinetic profiles of change in absorbance of $CHRA_3$ upon addition of DNA in the presence of Mg^{2+} were reported to resemble those for intercalating antibiotics such as actinomycin D (Behr et al., 1969; Li & Crothers, 1969; Shashiprabha, 1979).

Though the above studies have contributed to the understanding of certain aspects of $CHRA_3$–DNA interaction, they led to contradictory results regarding the molecular basis of the interaction. A major limitation of the results from most of these studies is that they tell very little about the role of Mg^{2+}. Furthermore, these studies were spread over a wide range of concentrations of Mg^{2+} from micromolar to millimolar levels. The antibiotic was shown to be anionic at and above physiological pH (Nayak et al., 1973; Illrionova et al., 1970). Accordingly, it was proposed that the role of Mg^{2+} is confined to acting as a counterion to bridge negative charges on the antibiotic and phosphodiester backbone of DNA (Waring, 1981). However, the following results are at variance with the above proposition: (i) $CHRA_3$ alone could bind to Mg^{2+} (Ward et al., 1965); (ii) affinity parameters (intrinsic binding constants and binding stoichiometry) for $CHRA_3$–DNA interaction were found to be dependent upon relative concentrations of Mg^{2+} and $CHRA_3$, even when Mg^{2+} is present above the stoichiometric concentration of $CHRA_3$ (Nayak et al., 1973, 1975); and (iii) chemical footprinting studies using MPE to identify the site of binding of the antibiotic to DNA (a restriction fragment) showed that there is a size and site dependence of the binding upon concentrations of $CHRA_3$ and Mg^{2+} (van Dyke & Dervan, 1983). It could, therefore, be proposed that the role of Mg^{2+} is not confined to a counterion only.

The above considerations led us to investigate the role of Mg^{2+} in $CHRA_3$–DNA interactions with the ultimate objective of understanding the molecular basis of the antibiotic–DNA interaction in the presence of Mg^{2+}. We approached the problem in two steps by systematic studies on the interaction of (i) $CHRA_3$ with Mg^{2+} and (ii) $CHRA_3$–Mg^{2+} complex(es) with DNA. This approach is justified because a knowledge of the molecular nature of the antibiotic–Mg^{2+} complex is required to understand the mode of (subsequent) interaction of the complex with DNA. The significance of this approach can be further appreciated if we consider that, under in vivo conditions, a $CHRA_3$–Mg^{2+} complex, instead of $CHRA_3$ alone, would be the species which binds to the cellular target DNA for inhibitory effects on macromolecular synthesis.

In this report, we present the results of optical spectroscopic studies, such as absorbance, fluorescence, and CD, on the above interactions. The first part of the study indicates formation of two types of complexes between $CHRA_3$ and Mg^{2+}. In the second part, we examined the binding potentials of these complexes with calf thymus DNA. The thermodynamic parameters associated with the interaction between these complexes and DNA were also evaluated to throw light on the molecular basis of the interaction. DNA from calf thymus was chosen as the natural DNA, because it consists of comparable percentages of AT and GC base pairs. Since an earlier report indicated that the pK_a of $CHRA_3$ is about 7.0 (Nayak et al., 1973), we carried out the present investigation at pH 8.0. It ensures a homogeneous population of negatively charged antibiotic molecules. Most of the earlier studies were also done at or near pH 8.0 (e.g., Nayak et al., 1973, 1975; van Dyke & Dervan, 1983; Keniry et al., 1987; Banville et al., 1990a,b; Shafer et al., 1988).

Materials and Methods

Chromomycin A_3 (a gift from Dr. R. H. Shafer of the University of California, San Fransisco), Tris, magnesium chloride solution (4.9 M), and calf thymus DNA were from Sigma Chemical Co. Unless mentioned otherwise, all studies were carried out in 20 mM Tris-HCl buffer, pH = 8.0. The buffer was prepared in triple-distilled (in all-quartz apparatus) deionized water. The concentration of $CHRA_3$ was estimated from its known extinction coefficient of 8.8 mM^{-1} cm^{-1} (at 405 nm) (Bakhara et al., 1968). Calf thymus DNA was deproteinized by the chloroform–phenol extraction method and precipitated with ethanol. It was then redissolved in 20 mM Tris-HCl buffer, pH = 8.0, extensively dialyzed against the same buffer containing 5 mM EDTA to remove divalent metal ions, and finally dialyzed against the buffer only to remove EDTA. The purity of DNA was checked and its concentration was determined spectrophotometrically.

Absorption, fluorescence, and CD spectra were recorded with a Hitachi U-2000 spectrophotometer, Hitachi F-4010 fluorometer, and Jasco J-500 spectropolarimeter, respectively. All fluorescence measurements for $CHRA_3$ and its complexes with Mg^{2+} were carried out at an excitation wavelength of 470 nm, instead of 405 nm (Shafer et al., 1988), because we observed a time-dependent decrease in fluorescence emission (by more than 50%) of the antibiotic (and its complexes with Mg^{2+}) upon excitation at 405 nm. On the other hand, no significant change (less than 2%) in emission intensity could

be detected upon excitation at 470 nm, a wavelength away from the peak (at 405 nm) in the absorption spectrum of free antibiotic (data not shown). Background emission (<5% at maximum) was corrected for by subtracting signals from blank buffer or DNA plus buffer samples. No correction was done for optical filtering effects, because absorbance of the samples (at 470 nm) never exceeded 0.02. The CAT mode, with the number of repeat scans between 4 and 8, was employed to record the fluorescence spectra. CD values were expressed in molar ellipticity: $[\theta] = (\theta_{obs} \times 100)/(cl)$, where θ_{obs}, l, and c denote the observed ellipticity (in millidegrees), path length of the cuvette (in centimeters), and molar concentration of the absorbing species, respectively. All spectra reported here are an average of two runs.

Measurement of Steady-State Fluorescence Polarization Anisotropy (FPA) $\langle r \rangle$. FPA was calculated from $\langle r \rangle = (I_{VV} - GI_{VH})/(I_{VV} + 2GI_{VH})$ (Cantor & Schimmel, 1981), where I denotes the intensity and the subscripts refer to vertical or horizontal positionings of excitation and emission polarizers, respectively. $G = I_{HH}/I_{HV}$ was used to correct for polarizing effects in the emission monochromator and detector. The excitation and emission wavelengths were 470 and 540 nm, respectively.

Analysis of Binding Data: (i) $CHRA_3$–Mg^{2+} Interactions. Spectrophotometric titrations of $CHRA_3$ with Mg^{2+} were analyzed as described earlier (Aich & Dasgupta, 1990). Fluorometric titration of $CHRA_3$ with Mg^{2+} was analyzed by means of the Stern–Volmer equation: $F/F_0 = 1 + K_q[Mg^{2+}]$, where F and F_0 denote the fluorescence emission intensity of $CHRA_3$ in the presence and absence of Mg^{2+}, respectively.

(ii) Ligand–DNA Interactions. Results from spectrophotometric titration to study the ligand (antibiotic–Mg^{2+} complex) interaction with DNA were analyzed in the following ways:

(i) Scatchard plot:

$$r/c_f = K_0(n - r) \quad (1)$$

where $r = c_b/c_p$ (c_b = concentration of bound ligand and c_p = concentration of DNA), n = binding stoichiometry in terms of bound ligand per nucleotide, and K_0 = intrinsic binding constant (Scatchard, 1949).

(ii) Li and Crothers type plot:

$$1/\Delta\epsilon = 1/\Delta\epsilon' + 1/[K\Delta\epsilon'(c_p - c_d)] \quad (2)$$

where $\Delta\epsilon = \epsilon_{obs} - \epsilon_f$ (ϵ_{obs} = apparent molar extinction coefficient of the bound ligand measured from the observed absorbance during titration, and ϵ_f = molar extinction coefficient of the free ligand), $\Delta\epsilon' = \epsilon_b - \epsilon_f$ (ϵ_b = molar extinction of the bound ligand), K = apparent binding constant ($K = K_0 n$), and c_d = concentration of ligand (Li & Crothers, 1969; Dasgupta & Goldberg, 1985). This equation is valid under the condition $c_p \gg c_d$, which is followed by keeping at least an 8-fold excess of DNA. For construction of Scatchard plots, the concentraton of the bound ligand, c_b, was evaluated from the relation

$$c_b = \Delta A/(\epsilon_b - \epsilon_f) \quad (3)$$

where ΔA denotes increase in absorbance of the ligand upon addition of DNA. Absorbance change at 440 nm was employed for construction of the above plots.

Dequenching of fluorescence of the ligand(s) as a function of added concentration of DNA was also analyzed to construct the binding isotherm according to the Scatchard method. The concentration of bound ligand (c_b) was calculated as follows: $c_b = (Q/Q_{max})c_{tot}$, where Q is the fractional dequenching during titration, Q_{max} is the fractional dequenching when the ligand is totally bound to DNA, and c_{tot} is the initial input concentration of the drug (Hard et al., 1989). Q is determined from the relation $Q = (I - I_0)/I_0$, where I_0 and I are emission intensities of the free and DNA-bound ligand (during the titration), respectively. Q_{max} is defined as $Q_{max} = (I_{max} - I_0)/I_0$, where I_{max} is the emission intensity of DNA-bound ligand. I_{max} is obtained from a plot of $1/I$ against $1/c_p$ (c_p = concentration of DNA) (Wang & Edelman, 1971); the resulting straight line is extrapolated to the y-axis, and the intercept on the y-axis gives the value of $1/I_{max}$. Thus known values of c_b, c_{tot}, and c_p allow us to construct the Scatchard plot according to eq 1. This approach is based on the assumption of a linear relation between emission intensity and concentration of the ligand, which we found to be valid up to $[CHRA_3] = 100\ \mu M$, corresponding to an excitation wavelength of 470 nm.

In the above cases, the experimental points for the binding isotherm were subjected to least squares analysis with a view to getting a best-fit straight line. For determination of binding parameters of the interaction between antibiotic–Mg^{2+} complexes and DNA, $CHRA_3$ was preincubated with Mg^{2+} for an hour at the desired temperature to make sure the formation of antibiotic–Mg^{2+} complex was complete. Small aliquots of DNA were then added to antibiotic–Mg^{++} complex and the equilibrium spectrum corresponding to addition of each aliquot was noted at the time when there was no further change in the spectrum with time. During the titration, total dilution due to addition of DNA was restricted to 5% of the initial volume, and correction due to dilution was incorporated in calculation of the binding parameters.

Determination of Thermodynamic Parameters. Thermodynamic parameters such as ΔF (free energy), ΔH (heat content), and ΔS (entropy) were evaluated using the following relations:

$$\Delta F = -RT \ln K \quad (4)$$

$$d \ln K/dT = -\Delta H/RT^2 \quad (5)$$

$$\Delta F = \Delta H - T\Delta S \quad (6)$$

where R and T are the universal gas constant and the absolute temperature, respectively (Castellan, 1989). For determination of ΔH, K was measured by means of eq 2 at three temperatures, 15, 25, and 32 °C. The slope of the best-fit line from the plot of ln K against $1/T$ gave the value of ΔH. Known values of ΔF and ΔH gave the value of ΔS.

Results

$CHRA_3$–Mg^{2+} Interaction. The change in the absorption spectrum of $CHRA_3$ upon addition of Mg^{2+} indicates formation of a complex between them (Figure 2). However, there are characteristic broadening and red-shifting of the peak accompanying the increase in input concentration of Mg^{2+} from 3.3×10^{-4} to 1.4×10^{-2} M (Figure 2). A similar trend in the change of the spectrum of $CHRA_3$ upon addition of millimolar concentrations of Mg^{2+} was reported earlier (Nayak et al., 1973). The observed difference in nature of the spectra of antibiotic–Mg^{2+} complexes formed at low and high concentrations of Mg^{2+} led us to carry out the spectrophotometric titration described below.

Absorbance of $CHRA_3$ (at 440 nm) was recorded as a function of the input concentration of Mg^{2+}. For the sake of clarity, the titration profile is shown in two parts in Figure 3. Panels a and b indicate the biphasic nature of the titration profile over the total range of input concentrations of Mg^{2+}. The first phase of titration corresponds to a range of concentration of Mg^{2+} from 0 to 3.7×10^{-4} M, while the second phase spans the concentration of Mg^{2+} from 3.7×10^{-4} to 1.3

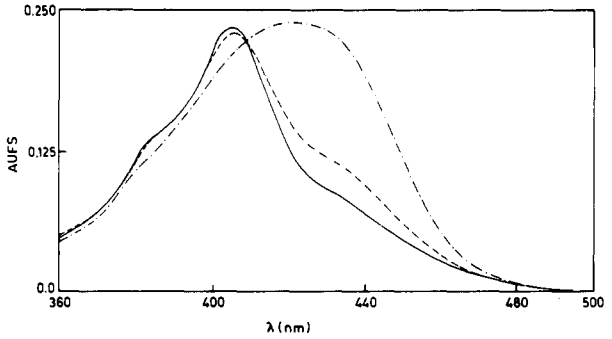

FIGURE 2: Absorption spectra in the visible region of $CHRA_3$ (2.6×10^{-5} M) alone (—) and in the presence of $[Mg^{2+}] = 3.3 \times 10^{-4}$ M (– – –) and 1.4×10^{-2} M(–·–), respectively, in 0.02 M Tris-HCl buffer, pH = 8.0, at 29 °C.

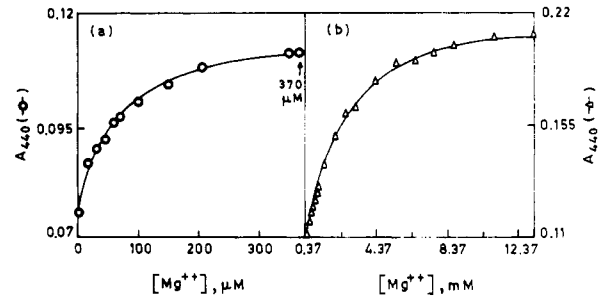

FIGURE 3: (a) Best-fit curve (based on 1:1 stoichiometry and association constant = 1.9×10^4 M^{-1}) for the experimental points (○) of spectrophotometric titration (at 440 nm) of $CHRA_3$ (2.95×10^{-5} M) with Mg^{2+}. $[Mg^{2+}]$ ranges from 1.5×10^{-5} to 3.7×10^{-4} M (in 0.02 M Tris-HCl buffer, pH = 8.0, at 29 °C). The number in the figure denotes the concentration of Mg^{2+} at the plateau. (b) Best-drawn curve through the experimental points (Δ) of spectrophotometric titration (at 440 nm) of $CHRA_3$ (2.95×10^{-5} M) with Mg^{2+}. $[Mg^{2+}]$ ranges from 3.7×10^{-4} to 1.3×10^{-2} M (in 0.02 M Tris-HCl buffer, pH = 8.0, at 29 °C). Please note that $[Mg^{2+}] = 2.0 \times 10^{-3}$ M corresponding to 50% of the total change in absorbance of $CHRA_3$.

$\times 10^{-2}$ M. There is an initial plateau corresponding to $[Mg^{2+}] = 3.7 \times 10^{-4}$ M and a final plateau at $[Mg^{2+}] = 1.1 \times 10^{-2}$ M. The biphasic nature of the titration curves leads us to propose that two different $CHRA_3$–Mg^{2+} complexes are formed over the range of input concentrations of Mg^{2+}. Figure 3a shows the best-fit curve (for the experimental points) based on 1:1 stoichiometry and an affinity constant of 1.8×10^4 M^{-1}. On the other hand, points shown in Figure 3b were analyzed by means of the concept of multiple equilibria as described for an analogous drug, mithramycin [MTR; Aich & Dasgupta, 1990]. The results, summarized in Table I, indicate 1.9:1 ($CHRA_3$:Mg^{2+}) stoichiometry for the complex described by the second phase of the titration. We obtained similar results also at 280 nm. The complexes corresponding to the first and second phases are termed complexes I and II, respectively. The spectrophotometric titration was repeated in a higher ionic strength buffer in order to assess the specificity of interaction associated with the formation of complexes I and II. The biphasic nature of the titration, akin to the profile observed in a low ionic strength buffer, suggests against nonspecific association (data not shown). The data were analyzed in the same way as above to conclude the formation of two complexes with 1:1 and 1.9:1 stoichiometry ($CHRA_3$:Mg^{2+}). There is, however, a reduction in the affinity constant for the formation of complex I (vide Table I).

$CHRA_3$ is optically active. Therefore, its chiral properties were examined as a function of added concentration of Mg^{2+} to verify the formation of two types of $CHRA_3$–Mg^{2+} complexes. CD spectra of $CHRA_3$, alone and in the presence of

Table I: Binding Parameters for $CHRA_3$–Mg^{2+} Interaction[a]

phase of titration curve	affinity constant (M^{-1})	stoichiometry ($CHRA_3$:Mg^{2+})
first	$(1.9 \pm 0.2) \times 10^{4}$ [b]	1:1
	8.0×10^{3} [c]	(1:1)
second	$(5.8 \pm 0.6) \times 10^{2}$ [b]	1.9:1
	5.6×10^{2} [c]	(1.8:1)

[a] The method for calculation of the parameters is mentioned in the text under Results. [b] The values are means of two sets of determinations in 20 mM Tris-HCl buffer, pH = 8.0, at 29 °C. Concentration of $CHRA_3$ is 2.95×10^{-5} M. [c] The titration was carried out in 200 mM Tris-HCl buffer, pH 8.0, at 29 °C.

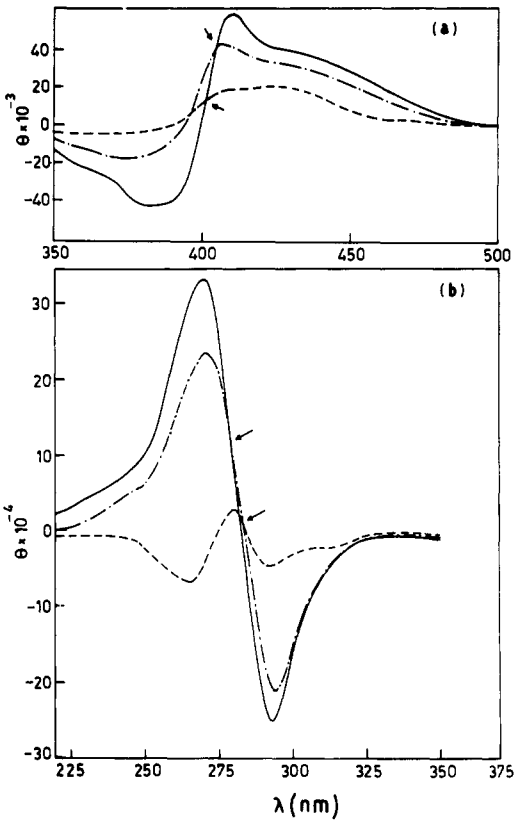

FIGURE 4: CD spectra of $CHRA_3$ (2.6×10^{-5} M) alone (—) and in the presence of Mg^{2+} at concentrations of 3.7×10^{-4} M (–·–) and 3.6×10^{-3} M (– – –), respectively, in (a) visible (350–500 nm) and (b) UV (220–350 nm) regions. Arrows indicate crossover points in the spectrum of free $CHRA_3$ and that of $CHRA_3$ in the presence of Mg^{2+}.

two concentrations of Mg^{2+}, are shown in Figure 4. It is noted from this figure that the spectra of the antibiotic–Mg^{2+} complexes across the spectrum of free antibiotic at different wavelengths; there is also a lack of similarity in the spectral profiles of the two complexes. The difference in nature of the spectra is more pronounced in the UV region. As shown in Figure 4b, there is an inversion of a band (in the 275–250-nm region) in the CD spectrum of free antibiotic upon addition of a concentration of Mg^{2+} which would favor the formation of complex II. These distinctive features in the chiral properties of the complexes could be ascribed to their different molecular structures. Similar trends were noticed from the examination of CD spectra of the antibiotic mithramycin and its complexes with Mg^{2+} (Aich & Dasgupta, 1990).

The above results bring forth a feature hitherto unreported for $CHRA_3$–Mg^{2+} interaction—the antibiotic forms two types of complexes with Mg^{2+} depending on the concentrations of $CHRA_3$ and Mg^{2+}. This is also the first direct evidence for formation of a 2:1 ($CHRA_3$:Mg^{2+}) complex in the presence

Table II: Steady-State Fluorescence Polarization Anisotropy (FPA) Values of $CHRA_3$ in the Presence of Mg^{2+} [a]

$[CHRA_3]$ (μM)	$[Mg^{2+}]$ (mM)	type of complex[b]	FPA ($\langle r \rangle$)
26			0.020
26	0.31	I	0.024
26	1.8	II	0.2

[a] The values were determined, as described under Materials and Methods, in 20 mM Tris-HCl buffer, pH = 8.0, at 29 °C. The antibiotic was preincubated with Mg^{2+} for 2 h to achieve equilibrium, after which FPA was measured. [b] The type of complex is identified from the spectrophotometric titration profile of $CHRA_3$ with Mg^{2+} (see text).

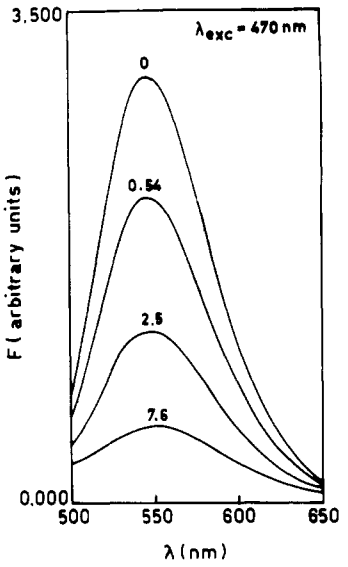

FIGURE 5: Change in fluorescence emission spectra of $CHRA_3$ (2.95×10^{-5} M) upon addition of Mg^{2+} in 20 mM Tris-HCl buffer, pH 8.0 at 29 °C. Numbers in the figure denote millimolar concentrations of Mg^{2+}. λ_{exc} denotes the excitation wavelength. Excitation and emission band-pass values were 3 and 10 nm, respectively. Please note that three representative spectra of $CHRA_3$ in the presence of Mg^{2+} are shown. A Stern–Volmer plot (see text) was obtained from a plot of fluorescence emission intensity at 550 nm against 12 different input concentrations of Mg^{2+} that ranged from 4.0×10^{-4} to 7.6×10^{-3} M.

of millimolar concentrations of Mg^{2+}. It is further supported from results of NMR studies of complex formation between $CHRA_3$ and oligonucleotide(s) in the presence of millimolar concentrations of Mg^{2+}. NOE and 2D-NMR data for the antibiotic–oligonucleotide complex(es) could be satisfactorily explained on the assumption of a $CHRA_3$–Mg^{2+} complex, with 2:1 stoichiometry, as the ligand which binds to the oligomer(s) (Banville et al., 1990a; Gao & Patel, 1990).

The fluorescence properties of $CHRA_3$ were employed to further probe the formation of different types of complexes and to throw light on their nature. We compared fluorescence polarization anisotropy (FPA) values of the free antibiotic and complexes I and II. The results in Table II show that there is an increase in the anisotropy due to formation of complex II. In contrast, there is very little change in the FPA (relative to the value for free antibiotic) asociated with the formation of complex I. This result provides additional evidence for the different molecular nature of complexes I and II. Considerable quenching of the fluorescence of $CHRA_3$ is associated with the addition of concentrations of Mg^{2+} which favor the formation of complex II (Figure 5). Quenching appears to be due to ground-state complex formation, because the quenching constant ($K_q = 3.4 \times 10^2$ M^{-1}) evaluated from a Stern–Volmer plot of the extent of quenching as a function of the input concentration of Mg^{2+} agrees well with the value determined

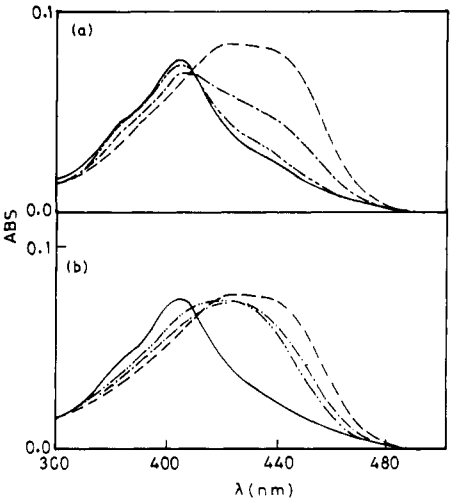

FIGURE 6: (a) Change in visible absorption spectra of $CHRA_3$ (9.0×10^{-6} M) plus Mg^{2+} (1.4×10^{-4} M) mixture (complex I) in the absence (—--—) and presence of DNA at concentrations of 3.3×10^{-5} M (—·—) and 2.3×10^{-4} M (---), respectively. The spectrum of free $CHRA_3$ (9.0×10^{-6} M) (—) is also shown for comparison. (b) Change in visible absorption spectra of $CHRA_3$ (9.0×10^{-6} M) plus Mg^{2+} (8.5×10^{-3} M) mixture (complex II) in the absence (—--—) and presence of DNA at concentrations of 2.8×10^{-5} M (—·—) and 2.3×10^{-4} M (---). The spectrum of free $CHRA_3$ (9.0×10^{-6} M) (—) is also shown for comparison. Please note that, in the text under Results, we have compared the absorption spectra of the antibiotic–Mg^{2+} complexes (---) in the presence of DNA at a concentration of 2.3×10^{-4} M.

from spectrophotometric titration (5.8×10^2 M^{-1}; vide Table I). In that case, a decreased quantum yield of complex II reflects an electronic environment of the chromophore (namely, the chromomycinone ring; see Figure 1) different from that in $CHRA_3$; this might originate from the presence of two chromomycinone rings in complex II.

Interaction of $CHRA_3$–Mg^{2+} Complex with DNA. Since complexes I and II are two different molecular entities, they would bind differently to the same DNA. The results of our experiments aimed at verifying this proposition are described below. It should be noted that, for the following experiments, concentrations of $CHRA_3$ and Mg^{2+} were chosen with the help of results from spectrophotometric titrations of $CHRA_3$ with Mg^{2+} so that they lead to formation of a single type of $CHRA_3$–Mg^{2+} complex (i.e., either complex I or complex II) and we do not get a mixed population of complexes I and II.

Progressive changes in the absorption spectra of complexes I and II upon addition of different concentrations of DNA suggest association between them and the polymer (Figure 6). Two common features of these changes are (i) red-shifting and broadening of the peaks and (ii) an increase in the absorbance beyond 410 nm of the spectrum of free $CHRA_3$. These features are consistent with earlier observations (e.g., Nayak et al., 1973; Shashiprabha, 1979). These features could be ascribed to the change in electronic environment of the chromomycinone ring of the antibiotic when the antibiotic–Mg^{2+} complex binds to DNA. Similar types of change in the absorption spectra characterize the association of ligands such as ethidium bromide and distamycin with DNA. A scrutiny of the spectra of complexes I and II in presence of near-saturating concentration (2.3×10^{-4} M) of DNA (Figure 6) shows that they are different in nature.

The fluorescence properties of complexes I and II were employed to study the binding between them and DNA. As shown in a representative example (Figure 7), dequenching of fluorescence of the ligand(s) occurs due to their interactions with DNA. The dequenching originates from a change in

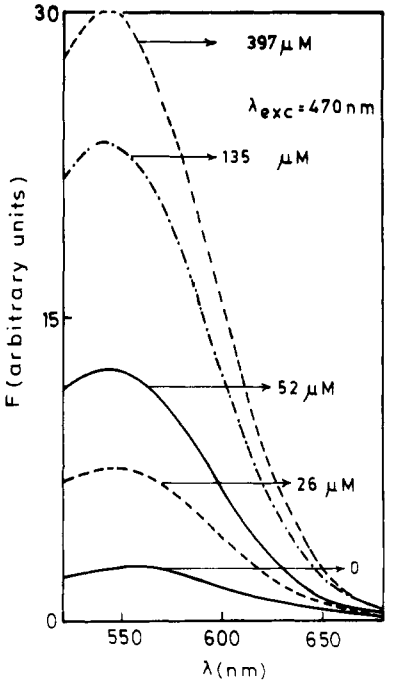

FIGURE 7: Change in fluorescence emission spectra of $CHRA_3$ (2.6×10^{-5} M) plus Mg^{2+} (2.1×10^{-2} M) mixture (complex I) in 20 mM Tris-HCl buffer, pH 8.0, at 25 °C upon addition of different concentrations of DNA indicated in the figure. λ_{exc} denotes the excitation wavelength. Excitation and emission band-pass values are 3 and 10 nm, respectively.

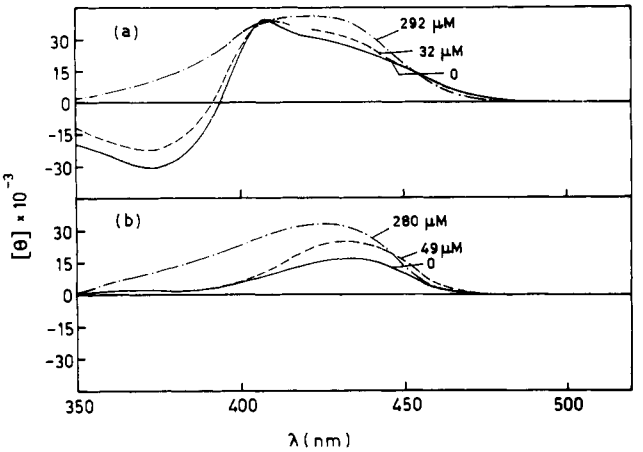

FIGURE 8: CD spectra (visible region) of $CHRA_3$–Mg^{2+} complexes containing (a) $[CHRA_3] = 2.7 \times 10^{-5}$ M and $[Mg^{2+}] = 2.5 \times 10^{-4}$ M (—) (complex I) and (b) $[CHRA_3] = 2.7 \times 10^{-5}$ M and $[Mg^{2+}] = 4.85 \times 10^{-2}$ M (—) (complex II) in 20 mM Tris-HCl buffer, pH = 8.0, at 32 °C upon addition of different concentrations of DNA as indicated in the figure.

either the local environment of the chromomycinone ring due to ligand–DNA interaction or the overall conformation of the ligand(s) upon binding to DNA. Both factors may also act in a concerted fashion, resulting in the dequenching. An increase in the fluorescence of the $CHRA_3$–Mg^{2+} complex at 575 nm (at an excitation wavelength of 405 nm) upon addition of poly(dG-me^{5}dC) was also reported earlier (Shafer et al., 1988). However, quantitation of the results from this study should be taken with skepticism because of the photosensitive nature of the antibiotic at 405 nm (see Materials and Methods).

CD spectra of $CHRA_3$–Mg^{2+} complexes (I and II) also change when they bind to DNA (Figure 8). A change in the CD spectrum of $CHRA_3$ as a result of interaction with DNA in the presence of millimolar concentrations of Mg^{2+} (Figure 8b) compares well with earlier reports (Shafer et al., 1988). While the disappearance of the negative band (in complex I) characterizes its association with DNA (Figure 8a), there is a considerable increase in intensity of the positive band for complex II upon binding to DNA (Figure 8b). Comparison of the spectra of DNA-bound complexes I and II (uppermost ones in Figure 8) shows that they have different profiles; e.g., the spectrum of DNA-bound complex I has a relatively broader band between 400 and 450 nm. It reinforces the observations (from the spectrophotometric titration shown in Figure 6) that the DNA-bound forms of complexes I and II have distinctive spectroscopic features.

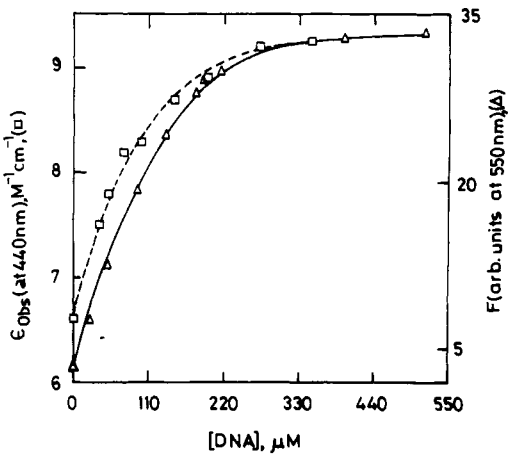

FIGURE 9: Plots of (i) apparent molar extinction coefficient (ϵ_{obs}) (□) at 440 nm of $CHRA_3$–Mg^{2+} complex I ($[CHRA_3] = 9.0 \times 10^{-6}$ M and $[Mg^{2+}] = 1.4 \times 10^{-4}$ M) and (ii) fluorescence emission intensity (Δ) at 540 nm of $CHRA_3$–Mg^{2+} complex I ($[CHRA_3] = 2.6 \times 10^{-5}$ M and $[Mg^{2+}] = 3.1 \times 10^{-4}$ M) against the concentration of DNA in 20 mM Tris-HCl buffer, pH = 8.0, at 25 °C.

Table III: Binding Parameters for $CHRA_3$–Mg^{2+} Complexes with DNA[a]

method	$[CHRA_3]$ (μM)	$[Mg^{2+}]$ (mM)	type of complex	K_0 ($\times 10^5$ M^{-1})	n (drug/nucleotide)
spectrophotometry	9.0	0.14	I	3.0 ● 0.1[b]	0.142[b]
	9.0	8.5	II	1.0	0.18
fluorometry	26.0	0.31	I	2.3	0.11[b]
	26.0	0.21	I	2.7	0.13
	26.0	21.0	II	1.8	0.18

[a] The values are in 20 mM Tris-HCl buffer, pH = 8.0, at 25 °C. They were evaluated by means of Scatchard plots as described under Materials and Methods. Concentrations of Mg^{2+} are chosen so that these would lead to formation of complex I (at lower concentrations of Mg^{2+}) or complex II (at higher concentrations of Mg^{2+}). [b] Average of the values from two sets of determinations with different batches of $CHRA_3$.

In order to check the nature of binding between the ligand(s) and DNA, the apparent extinction coefficient (at 440 nm) and fluorescence emission intensities (at 550 nm) of complexes I and II were plotted as a function of the input concentrations of DNA; the representative curves for complex I, as obtained from spectrophotometry and fluorescence titrations, are illustrated in Figure 9. The nature of the two curves indicates noncooperative binding between the ligand and DNA over the range of concentrations of DNA added. A similar trend was noticed for the titration curves representing interaction between complex I and DNA (data not shown).

We, therefore, used the above data to evaluate binding parameters, intrinsic binding constant and binding stoichiometry, for ligand–DNA interaction by means of Scatchard plots (see Materials and Methods). Representative plots for complex II–DNA interaction are shown in Figure 10. Collinearity of experimental points (obtained from spectrophotometry and fluorescence) is consistent with a noncooperative nature of

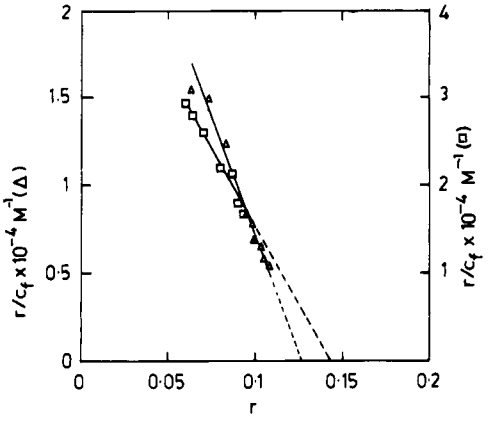

FIGURE 10: Scatchard plots in 20 mM Tris-HCl buffer, pH = 8.0, at 25 °C for interaction of complex II and DNA from spectrophotometric titration (□) at $[CHRA_3] = 9.0 \times 10^{-6}$ M and $[Mg^{2+}] = 1.4 \times 10^{-4}$ M and fluorometric titration (Δ) at $CHRA_3$ (2.6×10^{-5} M) and $[Mg^{2+}] = 2.1 \times 10^{-4}$ M.

Table IV: Apparent Binding Constant (K) for Interaction between $CHRA_3$–Mg^{2+} Complexes and DNA[a]

method	$[CHRA_3]$ (μM)	$[Mg^{2+}]$ (mM)	type of complex	K ($\times 10^4\ M^{-1}$)	ϵ_b (at 440 nm)[b] ($mM^{-1}\ cm^{-1}$)
spectrophotometry	9.0	0.14	I	3.45 (4.2)[c]	9.2
	9.0	8.5	II	1.6 (1.8)[c]	9.8

[a] The values are in 20 mM Tris-HCl buffer, pH = 8.0, at 25 °C. They were measured by means of eq 2, as described under Materials and Methods. [b] Evaluated from the reciprocal of the intercept on the ordinate in a plot such as that shown in Figure 11a. [c] Values in parentheses are apparent binding constants evaluated from K_o and n values in Table III by the relation $K = K_o n$. They are quoted for comparison.

interaction. Table III summarizes the relevant binding parameters evaluated from such plots. The following points are noted from the table. For the same concentration of $CHRA_3$, the binding parameters are different at two relative concentrations of Mg^{2+}. This is valid at both concentrations (9.0 and 26 μM, respectively) of $CHRA_3$. It supports the proposition that complexes I and II have different binding parameters for interaction with the same DNA. Binding parameters are also independent of the absolute concentrations of $CHRA_3$ and Mg^{2+}; on the other hand, the nature of the ligands (i.e., complexes I and II) determines the magnitude of their binding parameters. This could be concluded if we compare the binding parameters for the following sets of concentrations of $CHRA_3$ and Mg^{2+}: $[CHRA_3] = 9.0$ μM and $[Mg^{2+}] = 8.5$ mM, and $[CHRA_3] = 26.0$ μM and $[Mg^{2+}] = 21$ mM. For a ligand (complex I or II), there is an internal consistency of the results from spectrophotometric and fluorometric titrations, thus supporting the validity of the results obtained from them. An earlier study by spectrophotometry also indicated the dependence of binding parameters for $CHRA_3$–DNA interaction on the relative concentration of Mg^{2+} (Nayak et al., 1973). Present values compare well with the trend presented in this report. The difference in temperature and ionic strength of buffer at which these studies were done prevents a direct comparison of the values.

Apparent binding constants ($K = K_o n$) for interactions between complexes I and II and DNA were also determined by means of eq 2 from the change in their absorbance (at 440 nm) upon addition of excess DNA (vide Materials and Methods). Representative plots of $1/\Delta\epsilon$ against $1/(c_p - c_d)$ are shown in Figure 11a. The linear nature of the plots is consistent with an independent and noncooperative type of interaction. Relevant results are summarized in Table IV. Significant features of these results are as follows: (i) K values

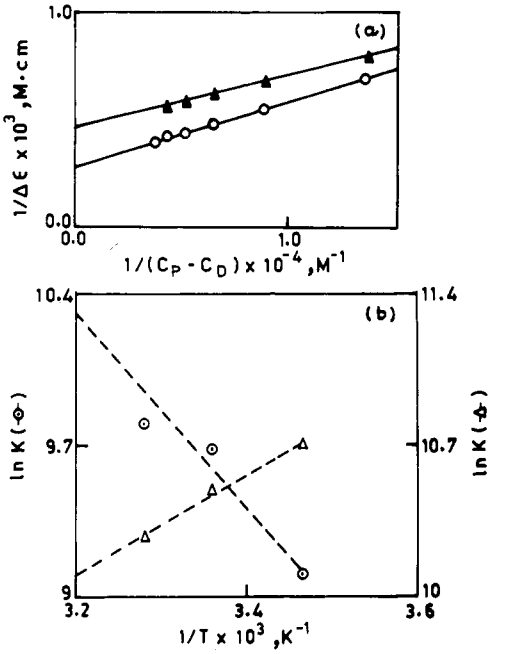

FIGURE 11: (a) Plots of $1/\Delta\epsilon$ against $1/(c_p - c_d)$ in 20 mM Tris-HCl buffer, pH = 8.0, for binding of complex II ($[CHRA_3] = 9.7 \times 10^{-6}$ M and $[Mg^{2+}] = 8.5 \times 10^{-3}$ M) at 15 °C (○) and 32 °C (▲), respectively. (b) Plots of ln K against $1/T$ for interaction between $CHRA_3$–Mg^{2+} complexes and DNA: complex I (at $[Mg^{2+}] = 1.4 \times 10^{-4}$ M) (△) and complex II at $[Mg^{2+}] = 8.5 \times 10^{-3}$ M) (⊙). The concentration of $CHRA_3$ is 9.0×10^{-6} M in both cases.

Table V: Thermodynamic Parameters for the Interaction between $CHRA_3$–Mg^{2+} Complexes and DNA[a]

type of complex	$[CHRA_3]$ (μM)	$[Mg^{2+}]$ (mM)	ΔF (kcal deg^{-1} mol^{-1})	ΔH (kcal/mol)	ΔS (eu)
I	9.0	0.14	−6.2	−4.8	4.8
II	9.0	8.5	−5.7	8.1	46.3

[a] The values are in 20 mM Tris-HCl buffer, pH = 8.0. Methods to evaluate them are described in the text.

listed in the table agree well with the value determined from the Scatchard equation, suggesting an internal consistency in the quantitation of the binding parameters. (ii) In line with the results presented in the previous paragraph, apparent binding constants for the same DNA are found to be different for complexes I and II. (iii) Molar extinction coefficients of DNA-bound complexes I and II are different. The last observation further validates the proposition that the DNA-bound forms of complexes I and II have distinctive spectral features; hence they are not identical.

Having established the influence of $[Mg^{2+}]$ upon the binding characteristics of the antibiotic with DNA, we attempted to measure the thermodynamic parameters for interaction between complexes I and II and DNA, with a view to providing a molecular basis of the observed dependence and, if possible, to throw light on the mode of interaction of $CHRA_3$–Mg^{2+} complexes with DNA. With this objective, K values for the interaction were determined (by means of eq 2) at three temperatures. Since we did not observe any dependence of binding stoichiometry on temperature (data not shown), we did not attempt evaluation of the intrinsic binding constant at different temperatures. A representative example of evaluation of K at two temperatures for complex I–DNA interaction is shown in Figure 11a. ln K was plotted against $1/T$, and ΔH values are calculated from the slope of the resultant straight lines, as illustrated in Figure 11b. Other thermodynamic parameters are calculated according to eqs

4 and 6. The values are summarized in Table V. The following features are indicated from the table. Binding of complex I to DNA is exothermic; in contrast, that of complex II to DNA is endothermic. Because of its endothermic nature, the later is an entropy-driven process.

Discussion

Major conclusions from the above results could be summarized as follows. $CHRA_3$ forms two types of complexes with Mg^{2+}, depending on the concentrations of the antibiotic and Mg^{2+}. These complexes are charaterized by differences in their absorbance, fluorescence, and CD spectroscopic properties. They have also different stoichiometries and association constants. These features indicate that their molecular structures are different. The recognition between these complexes and calf thymus DNA, in magnitude and nature, are not comparable.

The above conclusions are significant because they imply that, under physiological conditions, the antibiotic–Mg^{2+} complex(es), instead of the antibiotic alone, would bind to the prime cellular target, DNA and other potential sites, to exert the anticancer properties of the antibiotic. Each of the above findings is discussed separately to explain our results and correlate them with the earlier studies mentioned in the introduction.

$CHRA_3$–Mg^{2+} Interactions. Binding of the antibiotic to Mg^{2+} is characterized by changes in the optical spectroscopic properties of the antibiotic. A scrutiny of the metal ion dependence of the above change indicates formation of two types of complex. Formation of complex I is associated with a relatively smaller perturbation in the absorption and CD spectra of the free antibiotic. Absence of a major conformational change in free antibiotic due to formation of complex I could be suggested to account for this observation. Little change in anisotropy of complex I relative to that of free antibiotic further supports this proposition. It probably signifies that formation of complex I occurs via electrostatic and/or H-bonding interactions between the antibiotic and Mg^{2+}. The role of electrostatic interaction in the formation of this complex is further corroborated by the facts that (i) the antibiotic is anionic at experimental pH (Nayak et al., 1973) and (ii) there is a dependence of the formation constant of this complex on the ionic strength of the buffer (vide Table I).

On the contrary, we noticed significant changes such as (i) red-shifting and broadening of the absorbance peak, (ii) quenching of fluorescence emission intensity, (iii) an increase in the FPA, and (iv) inversion of a CD band in the UV region of the free antibiotic upon formation of complex II. The first two features could be ascribed to radical change in the electronic environment of the chromomycinone moiety in the antibiotic upon addition of millimolar concentrations of Mg^{2+}. Such radical change could occur as a sequel to a change in conformation of free antibiotic. The stoichiometry of complex II is consistent with this proposition, because one could envisage an interaction between two chromomycinone rings in a Mg^{2+}-coordinated dimer model for complex II. The interaction might contribute to the free energy of formation for complex II. This explanation is also consistent with the geometry of the ligand which was put forward to explain the 2D-NMR and NOE results of $CHRA_3$–oligonucleotide(s) complexes in the presence of millimolar concentrations of Mg^{2+} (Gao & Patel, 1990; Banville et al., 1990a). Stacking between two chromomycinone rings in complex II perturbs the energy for the $\pi \rightarrow \pi^*$ transition present in the free antibiotic, thus leading to the observed red shift, while the broadening might be due to relative hindrance to the motion of the overall molecule. It is further interesting to note that we observed a similar red shift and inversion of the CD band when the concentration of free $CHRA_3$ was enhanced to 900 μM, thus favoring self-aggregation (Hayasaka & Inoue, 1969). In the molecular aggregate, such as present in complex II, there can be deactivation of a singlet excited state leading to observed quenching and reduced quantum yield (Lakowitz, 1983). The altered Brownian motion of complex II, a bigger molecule, is probably responsible for the increase in FPA, though present data are not sufficient to do away with the possibility of the observed increase due to a change in lifetime of the excited state of complex II (Lakowitz, 1983).

The presence of sugar moieties in the antibiotic leads to the question whether they play a role in binding of Mg^{2+} to form two different complexes. In order to throw light on this aspect, we compared the values of formation constants of complexes I and II for $CHRA_3$ and the related antibiotic mithramycin (MTR; Aich & Dasgupta, 1990). MTR does not possess any acetyl or methoxy substitutes on sugar. A comparison indicates that, while the formation constant of complex I is comparable for $CHRA_3$ and MTR, the association constant for the formation of complex II is higher in the case of MTR (association constant = 1.6×10^3 M^{-1}). These results imply an involvement of sugar residues in the formation of complex II, because $CHRA_3$ and MTR contain different sugar residues. The pK_as of MTR and $CHRA_3$ are 5.0 and 7.0, respectively (Illrionova et al., 1970). At pH 8.0, both of them are predominantly anionic. The higher value of the association constant for complex II in the case of MTR could not be ascribed to the difference in their pK_a values. Further studies are, however, required to account for the above difference in affinity constants.

Interaction between $CHRA_3$–Mg^{2+} Complexes and DNA. Binding of complexes I and II to calf thymus DNA is indicated from changes in absorption, fluorescence, and CD spectra of the ligands. In order to check the specificity of interaction, the ionic strength of the medium containing an equilibrium mixture of either complex I or complex II and DNA was increased to 1 M NaCl. An insignificant change in the fluorescence emission properties of the mixture suggests against nonspecific interaction (data not shown). The red shift of the absorption peaks of the ligands upon their binding to DNA could be ascribed to perturbation of the $\pi \rightarrow \pi^*$ transition by the chromomycinone ring upon complexation with DNA. Comparison with similar red shifts observed for DNA-binding ligands, such as ethidium bromide (intercalator) or distamycin (groove binder), suggests that they might arise from either mode of binding, viz., intercalation or external binding. The proposition of change in electronic environment of the chromomycinone ring is corroborated from the observed dequenching of fluorescence of the ligands in the presence of DNA. A change in electronic environment could be due to the following factors: (i) There is a change in conformation of ligand(s), which may involve sugar residues. (ii) Microenvironments, such as local viscosity or hydrophobicity, of the chromomycinone ring are altered. (iii) Interaction with DNA leads to an enhancement in the extent of excited-state proton transfer, which was otherwise not facile in the drug–Mg^{2+} complex (Lepecq & Paoletti, 1967). The first two factors could also potentially lead to the observed change in chiral properties of the ligands when they bind to DNA.

Comparison of the nature of absorption and CD spectra of bound ligands (i.e., complexes I and II in the presence of DNA) and the difference in extrapolated values of ϵ_{obs} at 440

nm (vide Table IV) suggest that optical properties of the ligands, under the condition when they are bound to DNA, are different. It is consistent with the proposition that the bound ligands (i.e., DNA-bound complexes I and II) have different molecular structures.

Differences in binding and associated thermodynamic parameters characterizing the interactions between complexes I andII and DNA further support the view that they bind differently to DNA. As supporting evidence to the difference in binding stoichiometry of complexes I and II with DNA reported in the present study (vide Table III), results of chemical footprinting of $CHRA_3$ binding sites of restriction fragments containing promoter–operator region of lactose operon might be cited (van Dyke & Dervan, 1983). The concentrations of $CHRA_3$ and Mg^{2+} that were employed in this study would lead to formation of both complexes I and II. The results are relevant to indicate that antibiotic-protected regions increase in size at higher concentrations of $CHRA_3$ (100 μM) and Mg^{2+} (200 μM), which would favor formation of complex II. In contrast, less sites were reported to be protected at a lower concentration of $CHRA_3$ (25 μM) and Mg^{2+} (50 μM), which would lead to formation of complex I. The increase in binding stoichiometry observed from our study is consistent with this trend. On the other hand, hydroxyl radical footprinting was done under conditions (10 mM Mg^{2+}) which would lead to formation of complex II at all concentrations of $CHRA_3$ (Cons & Fox, 1989). That is why no site or size dependence of the binding on the concentration of antibiotic could be observed in this case.

The opposite nature of enthalpy changes associated with interactions of the ligands with calf thymus DNA is particularly significant as evidence for the different nature of the molecular recognition between the two complexes, I and II, and DNA. The possibility of difference in the conformation of DNA at different concentrations of Mg^{2+} as a source for the opposite nature of ΔH values was considered. It appears remote, because there has been so far no report of a gross change in B-DNA-type conformation as a sequel to binding of Mg^{2+} to the phosphate backbone (Zimmerman, 1982). Further, we did not notice any significant change in absorption of CD spectrum of calf thymus DNA over the range of input concentrations of Mg^{2+} used in the present study (data not shown). In order to account for the opposite nature of change in heat content, we also looked into the possibility that two complexes bind via different grooves (major and minor) of DNA. Our approach was 2-fold as stated here. We examined the ability of complexes I and II to substitute ethidium bromide, an established minor-groove-binding ligand, from DNA (Baguley, 1986) and we also compared the binding affinities of complexes I and II for two DNAs containing comparable percentages of GC bases but in one of which the major groove is blocked by a bulky substituent (Dasgupta & Goldberg, 1985). Results indicated that both ligands bind via the minor groove of DNA (P. Aich and D. Dasgupta, unpublished observations).

The negative change in enthalpy for complex I–DNA interaction is comparable to that for an intercalator like ethidium bromide (Wilson & Jones, 1982) or a groove-binding antibiotic such as distamycin (Zimmer & Wahnert, 1986). On the other hand, the positive change in enthalpy for complex II–DNA interaction probably indicates against an intercalative mode of binding, because a survey of literature shows that positive values of ΔH have so far been reported to be characteristic for external binding modes of the ligands to DNA (Dasgupta & Goldberg, 1986). An external binding mode was also indicated from ^1H NMR studies of $CHRA_3$–oligonucleotide(s) interaction in the presence of millimolar concentrations of Mg^{2+} (Gao & Patel, 1990; Banville et al., 1990a). A positive value of ΔH for complex II–DNA interaction could be ascribed to two plausible factors: (i) There is a change in conformation of the Mg^{2+}-coordinated dimer (i.e., complex II) upon complexation with DNA; the altered conformation is energetically not favorable, but it is stabilized by the interaction with DNA. (ii) Binding of the dimer to DNA induces a structural distortion of DNA from B-form at or near the binding site. Conformational change of complex II could be a potential origin for the observed increase in fluorescence. The second proposition is supported from ^1H-NMR studies reported earlier. These reports indicate a transition to non-B-DNA structure at binding loci of the $CHRA_3$–Mg^{2+} complex (type II) to oligonucleotide (Gao & Patel, 1990; Banville et al., 1990a). Footprinting studies also demonstrated that the analogous antibiotic MTR alters the structure of $(AT)_n$ sequences flanking the GC binding sites of the ligand (Cons & Fox, 1990). Higher stoichiometry of complex II (0.18 or 1 antibiotic molecule/2.5 base pairs, Table III), in spite of its bigger size, provides indirect evidence for a distorted structure from normal B-DNA at the binding site. A widening of the minor groove probably occurs to accommodate the Mg^{2+}-coordinated dimer.

Last but not the least important is the large difference in entropy change for interactions between these two ligands and DNA (vide Table V). The free energy change required for the interaction between complex II and DNA is largely derived from the entropy change (ΔS = 46 eu). Such a large change in entropy originates from the disordering of water molecules which are orderly placed along the minor groove of B-DNA (Dickerson et al., 1982). In contrast, the binding of complex I to DNA possibly does not perturb the hydration spine of DNA to a major degree. That is why the change in entropy is low.

Presently we are attempting to characterize the mode of binding of each type of complex with DNA and to compare their binding sites in a restriction fragment by footprinting analysis with a view to detecting a difference, if any.

Acknowledgments

We thank Professor (Dr.) N. Appaji Rao, Head of the Department of Biochemistry, Indian Institute of Science, Bangalore, India, for his permission to use the Jasco J-500 spectropolarimeter of the department. We also thank Professor (Dr.) P. K. Sengupta, Biophysics Division of SINP, for fruitful discussions on fluorescence measurements. D.D. and R.S. want to thank Professor (Dr.) M. K. Pal, Director of SINP, for his encouragement and permission to allow R.S. to work in this project in the Crystallography and Molecular Biology Division as a part of the training program for the M.Sc. course in biophysics, molecular biology, and genetics, University of Calcutta.

References

Aich, P., & Dasgupta, D. (1990) *Biochem. Biophys. Res. Commun. 173*, 689.

Baguely, B. C. (1982) *Mol. Cell. Biochem. 43*, 167.

Bakhara, G., Berlin, Y., Boldyreva, E., Chupronova, O., Kolosov, M., Soifer, V., Vasiljera, T., & Yartsera, I. (1968) *Tetrahedron Lett.*, 3595.

Banville, D. L., Keniry, M. A., & Shafer, R. H. (1990a) *Biochemistry 29*, 9294.

Banville, D. L., Keniry, M. A., Kam, M., & Shafer, R. H. (1990b) *Biochemistry 29*, 6521.

Behr, W., & Hartmann, G. (1965) *Biochem. Z. 343*, 519.
Behr, W., Honikel, K., & Hartmann, G. (1969) *Eur. J. Biochem. 9*, 82.
Berman, E., Brown, S. C., James, T. L., & Shafer, R. H. (1985) *Biochemistry 24*, 6887.
Calabresi, P., & Parks, R. E., Jr. (1985) in *The Pharmacological Basis of Therapeutics* (Goodman & Gilmann, Eds.) p 1247, Macmillan Publishing Co., New York.
Cantor, C. R., & Schimmel, P. R. (1980) *Biophysical Chemistry*, Part III, Freeman, San Fransisco, CA.
Castellan, G. W. (1989) *Physical Chemistry*, 3rd ed. (Indian student edition), p 799, Addison-Wesley, Reading, MA, and Narosa Publishing House, New Delhi.
Cobreros, G., Lopezzumel, M. C., & Usobiaga, P. (1982) *Radiat. Res. 92*, 255.
Cons, B. M. G., & Fox, K. R. (1989) *Nucleic Acids Res. 17*, 5447.
Cons, B. M. G., & Fox, K. R. (1990) *FEBS Lett. 264*, 100.
Dasgupta, D., & Goldberg, I. H. (1985) *Biochemistry 24*, 6913.
Dasgupta, D., & Goldberg, I. H. (1986) *Nucleic Acids Res. 14*, 3543.
Dickerson, R. E., Drew, H. R., Conner, B. N., Wing, R. M., Fratini, A. V., & Kopka, M. L. (1982) *Science 216*, 475.
Diel, H., & Lindstrom, F. (1959) *Anal. Chem. 31*, 414.
Fox, K. R., & Howarth, N. R. (1985) *Nucleic Acids Res. 13*, 8695.
Fox, K. R., & Waring, M. J. (1986) *Nucleic Acids Res. 14*, 2001.
Gao, X., & Patel, D. J. (1989) *Biochemistry 28*, 751.
Gao, X., & Patel, D. J. (1990) *Biochemistry 29*, 10940.
Gause, G. F. (1975) *Antibiotics*, Vol. III, p 197, Springer-Verlag, Berlin.
Goldberg, I. H., & Friedmann, P. A. (1971) *Annu. Rev. Biochem. 40*, 775.
Härd, T., Hsu, V., Sayre, M. H., Geidusschek, E. P., Appelt, K., & Kearns, D. R. (1989) *Biochemistry 28*, 396.
Hayasaka, T., & Inoue, Y. (1969) *Biochemistry 8*, 2342.
Illrionova, R. P., Dykhovichnaya, D. E., & Bondarenka, B. N. (1970) *Antibiotiki* (*Moscow*) *15*, 415.
Kam, M., Shafer, R. H., & Berman, E. (1988) *Biochemistry 27*, 3581.
Kaziro, Y., & Kamiyama, M. (1967) *J. Biochem.* (*Tokyo*) *62*, 424.
Keniry, M. A., Brown, S. C., Berman, E., & Shafer, R. H. (1987) *Biochemistry 26*, 1058.
Kersten, W., Kersten, H., & Szybalsky, W. (1966) *Biochemistry 5*, 236.
Lakowicz, J. R. (1983) *Principles of Fluorescence Spectroscopy*, p 257, Plenum Press, New York.
Lehninger, A. L. (1982) *Principles of Biochemistry*, p 779, Worth Publishers Inc., New York.
Lepecq, J. B., & Paoletti, C. (1967) *J. Mol. Biol. 27*, 87.
Li, H. J., & Crothers, D. M. (1969) *J. Mol. Biol. 39*, 461.
Lvashenko, V. A., & Kolesnicova, L. P. (1965) *Antibiotiki* (*Moscow*) *10*, 808.
Nayak, R., Sirsi, M., & Podder, S. K. (1973) *FEBS Lett. 30*, 157.
Nayak, R., Sirsi, M., & Podder, S. K. (1975) *Biochim. Biophys. Acta 378*, 195.
Scatchard, G. (1949) *Ann. N.Y. Acad. Sci. 51*, 660.
Schildkraut, C. L., Marmur, J., & Doty, P. (1962) *J. Mol. Biol. 4*, 430.
Shafer, R. H., Roques, B. P., Lepecq, J.-B., & Delepierre, M. (1988) *Eur. J. Biochem. 173*, 377.
Shashiprabha, B. K. (1979) Mode of action of antitumor antibiotic Chromomycin A_3, Ph.D. Dissertation, Indian Institute of Science.
van Dyke, M. W., & Dervan, P. B. (1983) *Biochemistry 22*, 2373.
Wakisaka, G., Uchino, H., Nakamura, T., Sotobayashi, H., Shirakawa, S., Adachi, A., & Sakurai, M. (1963) *Nature* (*London*) *198*, 385.
Wang, J. L., & Edelman, G. M. (1971) *J. Biol. Chem. 246*, 1185.
Ward, D. C., Reich, E., & Goldberg, I. H. (1965) *Science* (*Washington, D.C.*) *149*, 1259.
Waring, M. (1970) *J. Mol. Biol. 54*, 247.
Waring, M. J. (1981) *Annu. Rev. Biochem. 50*, 159.
Wilson, W. D., & Jones, R. L. (1982) *Intercalation Chemistry*, p 445, Academic Press, Inc., New York.
Zimmer, C., & Wähnert, U. (1986) *Prog. Bophys. Mol. Biol. 47*, 31.
Zimmerman, S. B. (1982) *Annu. Rev. Biochem. 51*, 395.